MRI-Compatible Device for Examining Brain Activation Related to Stepping

Martín Martínez, *Member, IEEE*, Federico Villagra, Francis Loayza, Marta Vidorreta, Gonzalo Arrondo, Elkin Luis, Javier Díaz, Mikel Echeverría, María A. Fernández-Seara, and María A. Pastor*

***Abstract*—Repetitive and alternating lower limb movements are a specific component of human gait. Due to technical challenges, the neural mechanisms underlying such movements have not been previously studied with functional magnetic resonance imaging. In this study, we present a novel treadmill device employed to investigate the kinematics and the brain activation patterns involved in alternating and repetitive movements of the lower limbs. Once inside the scanner, 19 healthy subjects were guided by two visual cues and instructed to perform a motor task which involved repetitive and alternating movements of both lower limbs while selecting their individual comfortable amplitude on the treadmill. The device facilitated the performance of coordinated stepping while registering the concurrent lower-limb displacements, which allowed us to quantify some movement primary kinematic features such as amplitude and frequency. During stepping, significant blood oxygen level dependent signal increases were observed bilaterally in primary and secondary sensorimotor cortex, the supplementary motor area, premotor cortex, prefrontal cortex, superior and inferior parietal lobules, putamen and cerebellum, regions that are known to be involved in lower limb motor control. Brain activations related to individual adjustments during motor performance were identified in a right lateralized network including striatal, extrastriatal, and fronto-parietal areas.**

***Index Terms*—Blood oxygen level dependent (BOLD) analysis, brain, dimensionality reduction, functional magnetic resonance imaging (fMRI), lower limbs movements, magnetic resonance imaging (MRI) compatible device, neural network.**

Manuscript received December 05, 2013; revised January 07, 2014; accepted January 13, 2014. Date of publication January 20, 2014; date of current version April 22, 2014. This work was supported in part by FIMA of the University of Navarra and in part by M.A.P Grant from FIS PI081949 and Navarra Government ref. 342005. *Asterisk indicates corresponding author.*

This paper has supplementary downloadable material available at http://ieeexplore.ieee.org, provided by the authors.

M. Martínez, F. Villagra, M. Vidorreta, G. Arrondo, E. Luis, and M. A. Fernández-Seara, are with the Neuroimaging Laboratory, Division of Neuroscience, Centre for Applied Medical Research (CIMA), University of Navarra, 31008 Pamplona, Spain.

J. Díaz was with the Neuroimaging Laboratory, Division of Neuroscience, Centre for Applied Medical Research (CIMA), University of Navarra, 31008 Pamplona, Spain. He is with the Electronic and Communications Department, Centre of Studies and Technical Research, 20018 San Sebastián, Spain.

F. Loayza was with the Neuroimaging Laboratory, Division of Neuroscience, Centre for Applied Medical Research (CIMA), University of Navarra, 31008 Pamplona, Spain. He is now with the Neuroimaging and Bioengineering Laboratory, Faculty of Mechanical Engineering, High Polytechnic School of Littoral (ESPOL), Guayaquil EC090150, Ecuador.

M. Echeverría is with the Department of Applied Mechanics, Centre of Studies and Technical Research, 20018 San Sebastián, Spain.

*M. A. Pastor is with the Neuroimaging Laboratory, Division of Neuroscience, Centre for Applied Medical Research (CIMA), University of Navarra, 31008 Pamplona, Spain (e-mail: mapastor@unav.es).

Color versions of one or more of the figures in this paper are available online at http://ieeexplore.ieee.org.

Digital Object Identifier 10.1109/TMI.2014.2301493

I. Introduction

HUMAN locomotion is a complex sensorimotor task that involves mainly the dynamic interaction of lower limb muscles acting on different joints, spinal locomotor pattern generators and a hierarchically coordinated network of brain structures distributed along the brainstem, cerebellum, basal ganglia, and cortex. This network controls movement and balance by integrating multisensory information enabling us to adapt our motor pattern with remarkable accuracy, speed, and versatility to environmental and subject-specific conditions [1].

The study of locomotion with functional magnetic resonance imaging (fMRI) is hampered by the difficulty of standing up in a high field scanner that would allow recording brain activity evoked by stepping, and the nature of the task itself. To address this limitation, several approaches have been proposed to provide indirect evidence of cortical involvement in locomotion. These approaches go from exploring brain activity patterns during imagined actions such as standing, walking, and running [2]–[6], to the assessment of active brain areas while performing voluntary or passive lower limb movements inside the scanner. The latter has been studied at diverse complexity levels: from the evaluation of isolated, unilateral, and repetitive ankle and knee movements [7]–[13] to more complex tasks that require coordinated movements of multiple joints such as pedaling [14] or stepping [15], [16].

While motor imagery-based studies, which are not hampered by movement-related artifacts, have provided valuable insight, they do not allow assessing neural activity associated with actual movements. On the other hand, alternating (anti-phase) and repetitive lower limb movements require internal pacing and inter-limb coordination, mechanisms that are also needed during locomotion and therefore have been proposed as a clinical surrogate of gait [2]. The advantages of this approach are that stepping movements can be performed in a supine position, allowing the study of evoked brain activation by means of fMRI or positron emission tomography (PET), provided that head movement is minimized [15], [16].

Quantitatively measuring the movement is crucial in fMRI experimental designs involving motor tasks [17] since brain activity has been shown to correlate with movement-dependent changes [18]. Yet, motor paradigms involving the lower limbs often do not quantify the behavior that underlies brain activity. Signal intensity changes from any voxel that arise from head motion represent a serious confound in fMRI, especially in motor control studies. To reduce task-related head movement, the use of MRI-compatible devices has been suggested as a

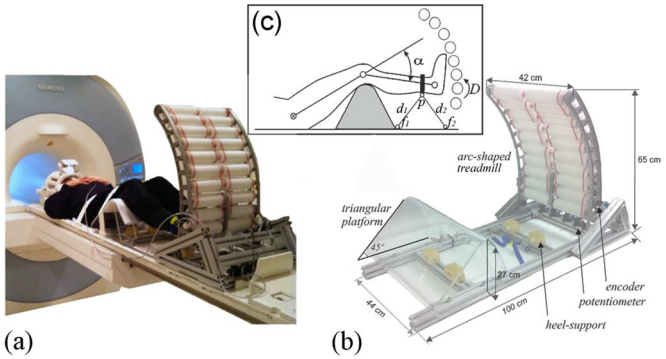

Fig. 1. (a) Set-up of the *pseudogait*-MRCD with a subject lying in the supine position on the scanner table. (b) Dimensions and components. (c) Diagram of design showing operating principles.

successful means of quantifying motor performance and at the same time facilitating isolated movements of the joints of interest with minimal head movement [11]. Another strategy employed to avoid excessive task-related movement artifacts, is the evaluation of brain activity in the rest period following the motor performance [14]. In order to prime the generation of rhythmical motion, an auditory or visual external stimulus is often employed to guide the participant's performance [7], [9], [16], [19].

In this work, we present a custom-designed *pseudogait*-magnetic resonance compatible device (*pseudogait*-MRCD) that facilitates the performance of cyclical and alternating lower limb movements inside the scanner bore. We have used blood oxygen level dependent (BOLD)-fMRI to assess the brain activation pattern associated with performing this task, in a group of healthy subjects. The *pseudogait*-MRCD was employed in order to help restrain the motion to the joints of interest while simultaneously registering the movement performed by the subjects. A visuo-spatial guide was designed to facilitate the generation of motion at a preset rate, while the choice of movement amplitude was left as a free parameter selected by the subject according to its own comfort. Simultaneous measurement of the lower limb kinematics, in terms of movement amplitude and frequency, allowed us to establish direct relationships between the BOLD signal and the concurrent motor behavior.

II. Materials and Methods

A. Instrumentation

1) Pseudogait-MRCD: We designed and manufactured a portable device aimed to facilitate the performance of alternating lower limb movements during fMRI testing while registering the displacements of knees and feet (Fig. 1). It was built with nonmagnetic metal and plastic (materials compatible with the MRI environment) and its total weight was 12 kg.

The structural design consisted of a vertical treadmill connected to a triangular methacrylate platform. The treadmill was formed by an arc-shaped structure comprising two independent columns of rollers. The position of the structure was adjustable along the exploration table according to the subject's height. The triangular platform was designed to restrain movement to the joints of interest. That is, it helped the subject to perform voluntary step-like movements and avoid hip movements while lying in the supine position. Moreover, it included a custom support to accommodate both heels [Fig. 1(b)]. The device allowed measuring the angle rotated by each knee (knee angle, or α) and the angular displacement (D) produced by the feet while moving the rollers during the task [Fig. 1(c)] by means of two protractors and two rulers (one for each leg).

Measuring α: Four cable potentiometers (UniMeasure LX-PA2.8-L1M, with a $\pm 1\%$ Full Scale linearity) were fixed to the triangular platform at the farthest distance from the scanner center to minimize their effect on the MRI signal. Two Velcro strips were placed around each of the subject's ankles. The free ends of two potentiometers cables were attached to the left Velcro strip at point p [Fig. 1(c)], and the other two remaining cables were attached to the right limb in the same manner. When a leg displacement was produced, point p described a circular trajectory centered about the knee of the subject. For each limb, the cables traveled from p to their corresponding potentiometer body passing through two fulcrums (f_1 and f_2), which were fixed to the aluminum structure in the plane containing the leg. When p changed its position, the potentiometers measured the distances d_1 and d_2—from f_1 and f_2 to p—. Once distances d_1 and d_2 were known, the x and y coordinates of p were calculated [20]. A direct measure of α was computed from the Cartesian coordinates of p (p_x and p_y) by a circular function (see (1) and Fig. 1(c) for more details)

$$\mathrm{tg}\,\alpha = \frac{p_y}{p_x}. \tag{1}$$

The measurement of α did not depend on the position of the fixation points, so the Velcro strips could be attached to each subject's lower limb at any position near the ankle.

Measuring D: The treadmill contained two columns of 10 cylindrical rollers per column manufactured with high molecular weight polyethylene (cestilene). The radius of each roller was 3 cm. When a movement was performed on one of the columns, rollers of that side turned together because they were interconnected with urethane belts. When the movement ended, the rollers stopped instantaneously due to the belt-system friction. The change in position produced by any movement at each roller-column was registered with an incremental optical encoder (Hewlett Packard HEDS-5540, with 10-bits resolution). In order to convert the registered values from the encoders to obtain a spatial measure (angular displacement, D in cm), the count registered with both sensors during one roller-turn was approximated to the perimeter of the roller.

The only electrical components of the device were the sensors and two shielded cables that connected the sensors to the Device Acquisition System (DAS), located outside the scanner room. The digitalized data from the device's sensors were filtered with a fifth-order Butterworth low-pass filter with a cutoff frequency of 5 Hz. The DAS converted the electric outputs from the *pseudogait*-MRCD to digital signals at a sampling frequency of 50 Hz by a data acquisition PCI card (Sensoray Model 626) installed in a PC. Finally, the PC executed a custom script implemented in MATLAB (R2009b, The Mathworks Inc., Natick,

MA, USA) which was linked to a block model designed in Real-Time Simulation Toolbox for Simulink (Simulation and Model Based Design Toolbox). Both tools allowed measurement and description of the kinematic behavior by means of the time series of α and D. The scanning session was synchronized with the DAS during the fMRI sequence with an optical trigger.

Information of measurement consistency check is described in the Supplementary Material, Section I.

2) Set-Up and Operation: Once inside the scanner, the subjects laid supine on the MR table, with both thighs placed on the triangular platform of the *pseudogait*-MRCD with knees flexed approximately 45°) and heels resting (Fig. 1). Arc-shaped pads were placed at the subject's heels to avoid artifactual motion when the subjects laid its feet on the support. In order to minimize head motion, a vacuum pillow (Siemens Cushion Head 4765454) was placed under the subject's head, whereas elastic Velcro straps were placed over the hips and thighs to further limit head motion as a consequence of lower limb movements.

Participants were requested to perform alternating stepping-like movements, where each isolated step of a limb comprised an upwards and downwards component. The upward movement was accomplished by an initial dorsiflexion of the ankle to avoid foot contact with the rollers, simultaneously with a progressive knee extension. Once the knee reached its maximum extension, the sole of the foot contacted the rollers initiating the downward movement, which was started by an ankle plantar flexion accompanied with a progressive knee flexion. During the downward movement, the foot contact with the rollers was maintained until the knee reached the position of maximal flexion entailing feet clearance and the start of a new step. Movements were restricted to the sagittal (vertical) plane.

Compatibility Study: As MR instrumentation and the subject's operation on the device (task-related motion) generate technical and image quality challenges, their influence on the MR environment should be previously tested. To this end, typical MRI evaluation measurements include image subtraction and signal-to-noise ratio (SNR) comparisons over the different conditions.

Regarding SNR measures, two variants are frequently used. Spatial SNR (sSNR) measures static image signal ratio over background noise; however it does not provide insight into the temporal noise characteristics of fMRI time courses. On the other hand temporal SNR (tSNR) is a useful measure of image intensity time course stability capable of detecting low-frequency temporal noise and false fMRI signals [21].

In the case of neuroimaging studies it is common to obtain the sSNR measure comparing the signal inside and outside a radiological phantom. Specifically sSNR is defined as

$$\mathrm{sSNR} = \frac{0.655 \times S}{\mathrm{SD}_{\mathrm{air}}} \tag{2}$$

where S is the mean signal in a ROI placed at the center of the phantom and $\mathrm{SD}_{\mathrm{air}}$ is the standard deviation of the signal well outside the phantom. *0.655* is a correction factor for characteristics of the noise distribution [22]. The sSNR was evaluated for each image in the time series.

tSNR is formulated for an image time series as the ratio of the mean signal over its temporal standard deviation. The tSNR was calculated for every voxel within the central ROI of the phantom

$$\mathrm{tSNR} = \frac{S_{\mathrm{voxel\_time\_series}}}{\mathrm{SD}_{\mathrm{voxel\_time\_series}}}. \tag{3}$$

We conducted a compatibility study in which a 50-scan time series of echo-planar images (EPI)* were acquired from a distilled water spherical head phantom (Siemens D170 of 170 mm diameter) under four different conditions.

Condition p_1: Phantom alone (baseline condition), with the *pseudogait*-MRCD located outside the scanner room.

Condition p_2: Phantom with the *pseudogait*-MRCD (no movement effect), with the device located on the scanner table.

Condition p_3: Phantom with the *pseudogait*-MRCD and movement, with the device on the table and with a person outside the scanner moving the rollers and the Velcro strips at the preset task rate.

Condition p_4: Phantom alone (second baseline condition). * The parameters of the EPI sequence used during the phantom-study were identical to those used during the fMRI study and are described in Section II-B2).

In order to minimize environmental changes in the scanner room, all the experimental conditions were recorded within the same session moving neither the scanner table nor the phantom between conditions. To estimate the effect of introducing the *pseudogait*-MRDC, its motion and scanner instabilities, we evaluated the differences in the mean images of each condition (by performing direct voxel-wise subtraction of the control p_1 condition from conditions p_2, p_3, and p_4) and quantified the percent change in brightness in the difference images. We also determined the SNR and tSNR for each condition. Results were compared with a Kruskal–Wallis test performed in MATLAB.

B. fMRI Study

1) Subjects: Nineteen right-handed [23] volunteers (nine women; age 33±5 years, height 168±8 cm, weight 69±12 kg; mean±SD) without any history of neurological, motor or cardiovascular disorder were recruited among the personnel of the University of Navarra. Prior to their participation, all subjects signed a written informed consent.

2) Scanning Protocol: The study was carried out using a 3T scanner (Siemens Trio TIM, Siemens AG, Erlangen, Germany) equipped with a 12-channel head array coil. It consisted of one session that included the acquisition of an anatomical dataset and the functional run, with a total duration of 15 min. The anatomical T1-weighted image was acquired with a MPRAGE sequence of 5 min duration. The following imaging parameters were employed: 1-mm isotropic resolution, $\mathrm{FOV} = 256 \times 192$ mm^2, $\mathrm{matrix} = 256 \times 192$ voxels, 160 axial slices, repetition time/echo time $(\mathrm{TR/TE}) = 1620/3.09$ ms, Inversion Time $(\mathrm{TI}) = 950$ ms, $\mathrm{flip\ angle} = 15°$. During the functional run, a total of 240 imaging volumes sensitive to BOLD contrast were acquired using a T2*-weighted EPI sequence. Each volume comprised 36 transverse slices of 4 mm thickness with a 0.2 mm gap. Other imaging parameters were: $\mathrm{resolution} =$

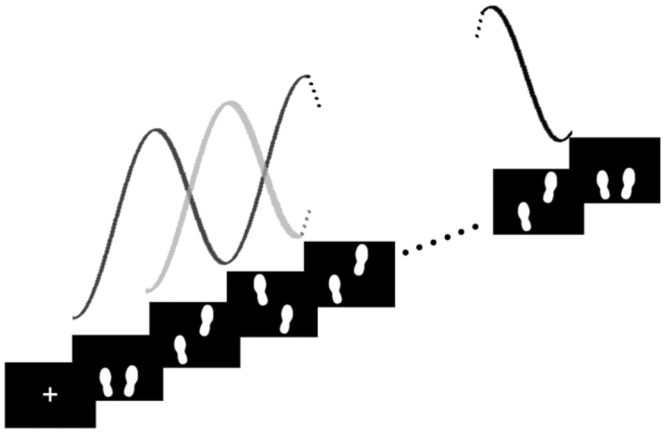

Fig. 2. Motor paradigm employed in the study with a visuo-spatial guide indicating the evolution of the spatial pattern of the cues in the sagittal plane. The stepping frequency used in the study was equivalent to a period of 0.83 s.

3×3 mm^2, FOV $= 192 \times 192$ mm^2, matrix $= 64 \times 64$ voxels, TE $= 24$ ms, TR $= 2.0$ s.

3) Functional Paradigm: The motor paradigm interleaved 10-s blocks of voluntary alternating strides of the lower limbs (stepping condition, or SC) and 30-s blocks of rest (control condition, or CC). External visual guidance was included to assist the subjects in achieving a rhythmical pattern. Cues consisted in two footsteps that moved vertically and alternatively at 1.2 Hz. The sequence started with the right foot, whereas each footstep reversed its trajectory upon reaching the top and bottom endpoints (Fig. 2). Finally, after five repetitions, one of the feet did not finish its corresponding stride and went back to the initial position, indicating to the subject that the block was ending. Video-animated frames were generated in Adobe Flash Professional and projected onto a screen behind the subject's head that was visible through a mirror clamped to the head coil.

A fixation cross appeared at the center of the screen just before the start of SC indicating that a stepping block was about to start. During the SC subjects had to take steps using the pseudogait-MRCD following the pace of the visual guide. However, participants were free to choose the amplitude of their strides. During the CC subjects were instructed to relax with eyes open while maintaining their feet on the heels-support. In order to minimize visual effects of no interest on brain activity, the visual stimulus was maintained across conditions (with the exception of the color which was white in SC and yellow in CC). Each condition was repeated 12 times with a final total duration of 8 min. Eye-tracker data were continuously recorded, for control of attention and sleepiness. Before the scanning session, subjects practiced the paradigm outside and inside the scanner until they achieved a comfortable coordinated lower limb pattern. Investigators also explained the importance of keeping the head still inside the scanner. During the fMRI scan, the α and D measurements were continuously recorded.

4) Data Analysis:

a) Kinematic Data Analysis: Table I describes the kinematical features of the participants motor behavior, which were estimated from the α and D time profiles.

TABLE I
DESCRIPTION OF THE KINEMATICAL FEATURES ASSESSED DURING THE MOTOR PERFORMANCE

Feature	Acronym	Unit	Description
Knee stepping frequency	SK_k	Hz	Frequency of successive knee extensions over a SC block
Stepping amplitude	SA	degrees	Total angle rotated by each knee (extension + flexion) during a step
Asymmetry coefficient	AC	-	Ratio between right and left SAs
Total extent of movement	TEM	degrees	Total displacement over a SC block (sum of right and left SAs)
Feet stepping frequency	SF_f	Hz	Frequency of successive contacts of the feet with the rollers over a SC block

First, the individual left and right knee extension-flexion times were identified from the peaks of their respective α temporal profiles. The knee stepping frequency ($\mathrm{SF_k}$, in Hz) was defined as the inverse of the time between successive knee extensions. The stepping amplitude (SA, in degrees) was computed as the sum of the knee extension and flexion angles within a step. Also, an asymmetry coefficient (AC) was defined as the spatial ratio between right and left SAs. This parameter reflects angular differences between right and left knee displacements, so in a totally symmetric movement, AC should be 1. Finally, the total extent of movement (TEM, in degrees) was computed as the sum of right and left SAs over a whole *SC* block.

Next, feet temporal features were extracted from the temporal profile of D. The rollers velocity was derived from D and it allowed identifying the initial contact of each foot with the roller system, and likewise its separation from the rollers after each step. The foot stepping duration was calculated as the time elapsed between successive contacts of the feet with the rollers, and feet stepping frequency ($\mathrm{SF_f}$, in hertz) was defined as the inverse of the feet stepping duration.

All measures were extracted for each *SC* block and subsequently averaged across repetitions using custom scripts in MATLAB (R2009b, The Mathworks Inc., Natick, MA, USA).

The last two movements corresponding to the end of each SC were discarded since they were not complete steps. Kinematic features were averaged over SCs to obtain a representative value for each subject. As subjects chose their preferred SA, we carried out a multiple regression analysis in MATLAB to determine whether this feature was correlated with any of the demographical features (sex, age, height, and weight) of the population. A p-value $p < 0.05$ was considered statistically significant.

b) Imaging Data Analysis: b.1) Preprocessing: Image preprocessing and analysis were performed using Statistical Parametric Mapping (SPM8) (Statistical Parametric Mapping software, SPM: Wellcome Department of Imaging Neuroscience, London, U.K.; http://www.fil.ion.ucl.ac.uk/spm/) and custom scripts implemented in MATLAB. For each subject, functional EPI volumes were realigned to the session mean volume using SPM8 motion correction algorithm [24]. The Artifact Repair toolbox (ver. 5, [25]) was employed to detect and eliminate artifacts from realigned images. The motion threshold was set to 0.5 mm/TR and artifact volumes were replaced with the average of their adjacent scans. We decided

a priori that any session with artifacts in more than 10% of the volumes would be discarded. Realigned data volumes were co-registered to the individual anatomical image and spatially normalized to the MNI template (Montreal Neurological Institute) based on ICBM-152 coordinates [26] using the parameters determined by the combined segmentation and normalization of the T1-weighted image [27]. A Gaussian filter of 8-mm full-width at half-maximum (FWHM) was applied to spatially smooth the data.

b.2) Statistical Analyses: To evaluate BOLD signal differences across conditions, a statistical inference analysis was performed in the context of the General Linear Model (GLM, [28]). Voxel-wise statistical analysis was performed for each subject in a block design that modeled both SC and CC conditions—using a boxcar function convolved with the SPM8 hemodynamic response function—after smoothed data volumes were time-filtered using a high-pass filter of 0.008 Hz to remove the slow signal drifts with a period longer of 128 s that are related to scanner and physiological noise. The movement parameters extracted from the realignment were not included in the design matrix to avoid the deleterious impact on sensitivity when motion and the experimental task design are correlated [29]. The contrast of interest comparing SC to CC was estimated individually with a fixed-effects model and followed by a group inference using the random effects model [30]. To evaluate the effect of incorporating in the analysis the actual kinematic data recorded during the subject performance, this analysis was replicated including as covariate at the subject level the computed TEM of each SC block. Introducing this covariate allowed controlling for possible variations in motor behavior across blocks.

A final analysis at the group level was performed including the mean and variance of each subject's SA as regressors, in addition to the contrasts maps derived from the first level analysis. The first covariate aimed to address changes in neural activity correlated with the different degree of lower limb displacements, while the variance was introduced as a nuisance variable. We generated two group t-maps, 1) testing for brain activity related to stepping (differences between SC and CC), and 2) testing for activation positively correlated with the SA using one-sample t-tests for the specific contrast parameter in the design matrix.

A $p < 0.05$ FDR cluster-wise correction was employed to correct for multiple comparisons, after a voxel level uncorrected significance threshold of $p < 0.001 (T = 3.69)$.

III. Results

A. Compatibility Study

Fig. 3 shows the results of the MRI compatibility test on the head phantom. In Fig. 3(a) the mean images of the experimental conditions p_1, p_2, p_3 and p_4 are depicted in the two left columns, while the third column shows the difference images across conditions resulting from direct voxel-wise subtraction. We observed a 2.5%, 1.9%, and 3.07% change in the average brightness between conditions p_2 and p_1 (Fig. 3(a), first row), p_3 and p_1 (Fig. 3(a), second row) and p_4 and p_1, (Fig. 3(a), third row), respectively. When we compared conditions p_2 and p_3 to estimate the effect of movement (performed at a distance from the phantom) (Fig. 3(a), third row), we observed a change in the average brightness of 0.9%.

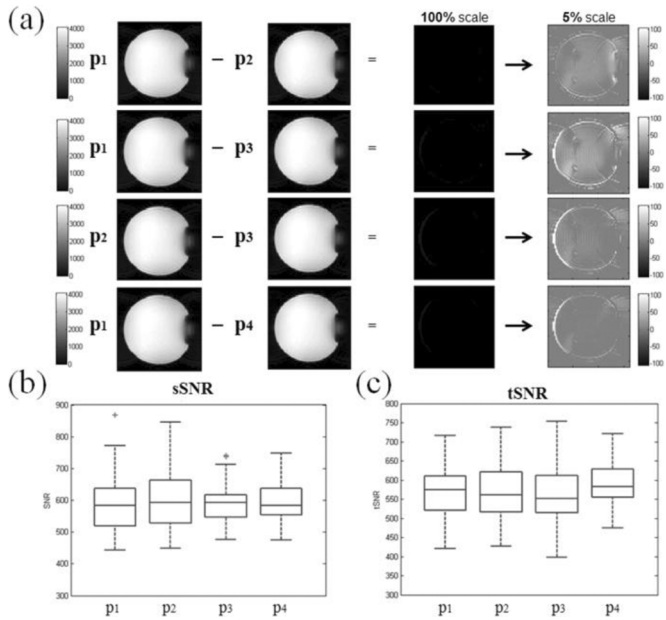

Fig. 3. Compatibility assessment of the pseudogait-MRCD. (a) Mean images of the phantom during the different conditions (p_1: phantom alone (baseline condition), p_2: phantom with the device, p_3: phantom with the device and a person simulating subject's step-like movements) and p_4: phantom alone (second baseline) and pair-wise subtraction of the condition images, displayed at full scale and 5% scale, (b) sSNR values for all the images in the time series and, (c) tSNR values for all the voxels within the phantom central ROI, across experimental conditions. There were no significant statistical differences between conditions.

These changes were visually imperceptible when displayed on the original brightness scale. When the scale was increased to 5% of its original value, we observed systematic brightness changes and a ghosting effect around the contour of the phantom (Fig. 3(a), forth column). Fig. 3(b) and (c) shows the mean and the standard deviation values of the sSNRs and tSNRs calculated under each condition. The Kruskal–Wallis tests evaluating the differences in sSNR and tSNR across conditions failed to reach significance ($p_{\mathrm{sSNR}} = 0.97$ and $p_{\mathrm{tSNR}} = 0.122$). Results indicate that signal changes produced by the introduction and operation of the *pseudogait*-MRCD and from scanner instabilities were of negligible relevance.

B. Behavioral Study

1) Motor Performance: The motion parameters registered at knees and feet corroborate that participants were able to perform the requested alternating lower-limb movements during the SC, with precise foot contacts on the treadmill of the *pseudogait*-MRCD (see Fig. 4(a) and (b) for a time profile sample recorded at the knee (α) and the feet displacement (D) of a representative subject during all SCs). That is, the registered profiles reflected an anti-phase coordination pattern during the task performance, similar to gait. We observed high inter-subject variability in the SA feature, with the group mean being $\mathrm{SA} = 45.25 \pm 17.21°$ [Fig. 4(c)], which meant that each individual self-adjusted the SA of the movements while keeping the

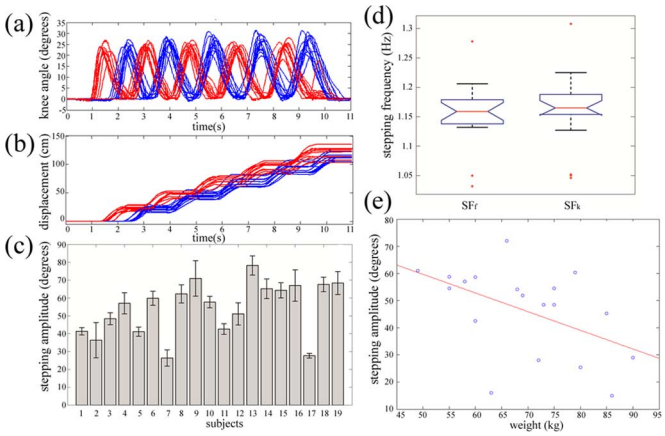

Fig. 4. (a) Time series of α and, (b) D during all SC blocks (superimposed) of a representative subject (red and blue curves represent the right and left knee displacements, respectively), (c) individual stepping amplitude (SA), (d) boxplots of the group stepping frequency during task at feet $(\mathrm{SF_f})$ and knees $(\mathrm{SF_k})$ and (e) negative linear correlation between the SA and weight.

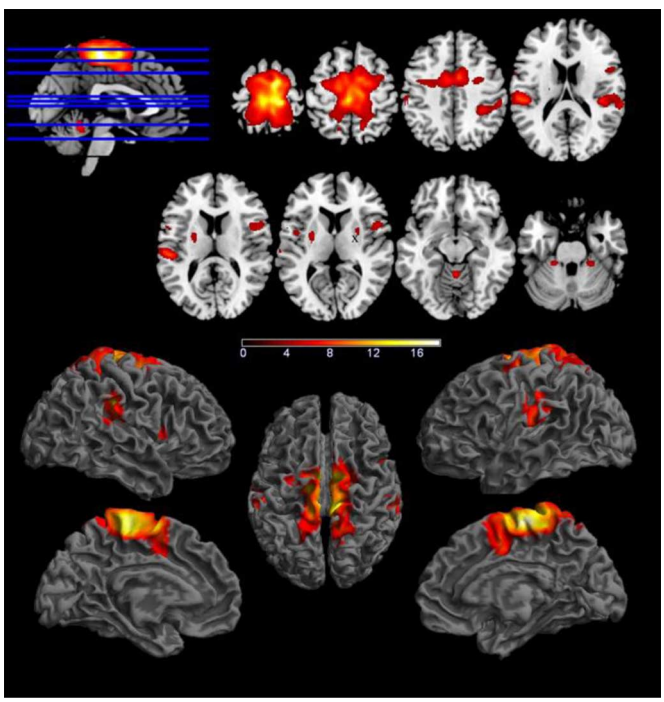

Fig. 5. Regions of the brain activated during the stepping task, superimposed on a two-(top) and three-dimensional (bottom) standard brain. Signal changes were considered significant at $p < 0.001$ and corrected for multiple comparisons by FDR at the cluster-level $(\mathrm{k} = 130)$. X: Cluster not surpassing the threshold for multiple comparisons. Color scale represents statistical T-values.

pace close to that of the visual guide. The group average stepping frequencies of knee and foot were $\mathrm{SF_k} = 1.16 \pm 0.06$ Hz and $\mathrm{SF_f} = 1.15 \pm 0.05$ Hz, respectively, as shown in Fig. 4(d). Moreover, the knee and feet showed similar but not equal coordination during the stepping motion, as reflected in Fig. 4(d) by the different variability (more information in Supplementary Material, Section II). These results confirmed that participants closely matched the pattern imposed by the visuo-spatial guide, with a pace set at 1.2 Hz.

The group AC (reflecting the ratio between right and left limb displacements) was 1.06 ± 0.103 and the group TEM was $478.16 \pm 30.1°$. Finally, the multiple regression analysis showed a significant negative correlation $(\mathrm{r} = -0.42, \mathrm{p} = 0.04)$ between the SA and the subjects' weight, as reflected in Fig. 4(e).

TABLE II
MNI COORDINATES FOR ANATOMICAL AREAS THAT SHOW MAXIMUM ACTIVATION FOR GROUP ANALYSIS ASSOCIATED WITH STEPPING

REGION	CLUSTER SIZE VOX.	SIDE	MNI COORDINATES X	Y	Z	STAT. VAL.T
PARACENTRAL LOBULE (BA4)	28225	R	6	-25	63	18.19
		L	-6	-27	63	16.74
PRECENTRAL GYRUS (BA4A)		R	15	-30	69	16.69
SUPERIOR FRONTAL GYRUS (BA6)		R	23	-9	60	12.66
SUPRAMARGINAL GYRUS (BA48)	3426	L	-54	-25	15	10.74
SUPERIOR TEMPORAL GYRUS (BA22)		L	-61	-21	12	4.71
SUPRAMARGINAL GYRUS (BA2)	3401	R	56	-30	31	11.14
INTRAPARIETAL SULCUS (BA40)		R	36	-39	40	6.50
PRECENTRAL GYRUS (BA4)	1135	R	51	8	31	6.49
INFERIOR FRONTAL GYRUS, P. OPERCULARIS (BA48)		R	53	9	9	5.61
CEREBELLAR VERMIS (LOBULES I-IV (HEM))	400	R	2	-48	-14	6.14
CEREBELLUM HEMISPHERE (LOBULE V)		L	-21	36	-27	5.57
CEREBELLUM HEMISPHERE (LOBULES I-IV)		L	-11	40	-21	4.62
PUTAMEN	224	L	-26	-4	10	5.64
CEREBELLUM (LOBULE V)	130	R	24	-36	-29	5.20
PRECENTRAL GYRUS (BA6) *	105	L	-57	4	24	6.43
INSULA (BA13-16) *	82	L	-45	0	7	4.56
MIDDLE FRONTAL GYRUS (BA46) *	76	R	35	47	22	4.61
ROLANDIC OPERCULUM (BA48) *	58	L	-56	8	3	4.83
PUTAMEN *	54	R	27	3	7	4.17
INFERIOR FRONTAL GYRUS, P. OPERCULARIS (BA6) *	30	L	-57	8	13	4.08

Signal changes were considered significant at $p < 0.001$ and corrected for multiple comparisons by FDR at the cluster-level (k = 130; R, right, L, left; BA, Brodmann Area). * These areas were observed at $p < 0.001$ uncorrected voxel threshold, however due to their cluster size, values did not survive cluster-wise correction.

2) Neural Activity Associated With Stepping:

a) Stepping vs. Rest: Head motion remained under 3 mm for all the subjects (for further details, see Supplementary Material, Section III). Therefore, no subjects or sessions were discarded from the study due to excessive artifacts from head motion. At the subject level, the inclusion of the TEM parameter as a covariate resulted in an increase of significance in the contrast maps obtained in the comparison of SC versus CC. Additionally, the statistical significance of the resulting group contrast map was also increased when including the subjects' SA mean and variance as covariates in the analysis at the group level. The results showed that the brain network activated by stepping included bilaterally primary motor cortex (M1), premotor cortex (PMC), supplementary motor area (SMA), and medial cingulate cortex (MC), primary and secondary somesthetic cortices, and bilateral areas in the inferior parietal lobule (IPL) and superior parietal lobule (SPL) including precuneus.

Significant subcortical activations were also found bilaterally in the putamen (greater in the left hemisphere), vermian, and somesthetic hemispheric cerebellar cortex (Fig. 5 and detailed information in Table II).

b) Brain Activity Correlated With the Stepping Amplitude: The contrast map resulting from the group analysis showed brain activity positively correlated with the SA in several

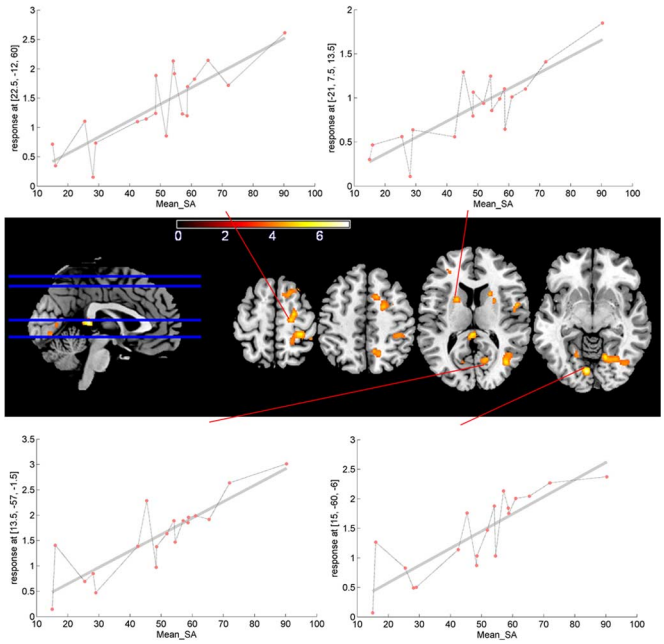

Fig. 6. Brain regions correlating with the SA. Signal changes were considered significant at $p < 0.001$ and corrected for multiple comparisons by FDR at the cluster-level ($k = 172$). Color scale represents statistical T-values. Charts above and below represent the positive correlation between the BOLD signal and the SA in some specific brain regions.

regions including the bilateral primary and associative visual cortex:, the lingual gyrus, the right middle temporal complex (hOC5/V5); the right superior postcentral gyrus extended to the supramarginal gyrus and to the inferior parietal lobule, the right superior parietal lobule, the right medial cingulate cortex, the bilateral pre supplementary motor area, the right supplementary motor area, the right premotor cortex, the right precentral gyrus, the right Rolandic operculum, the left dorsolateral prefrontal cortex, the right caudate nuclei and the bilateral dorsal putamen (Fig. 6 and detailed in Table III).

TABLE III
COORDINATES (IN MNI STANDARD BRAIN SPACE) OF THE ANATOMICAL AREAS SHOWING SIGNIFICANT POSITIVE CORRELATIONS WITH THE STEPPING AMPLITUDE COVARIATE

REGION	CLUSTER SIZE VOX.	SIDE	MNI COORDINATES X	Y	Z	STAT. VAL.T
LINGUAL GYRUS (BA18)	2746	R	12	-58	0	7.14
INFERIOR TEMPORAL GYRUS (BA19)		R	42	-70	-5	5.39
MIDDLE TEMPORAL GYRUS (BA37)		R	41	-69	13	5.25
FUSIFORM GYRUS (BA19)		R	30	-66	-9	5.16
CALCARINE GYRUS (BA17)		R	-9	-70	16	4.75
SUPERIOR FRONTAL GYRUS (BA6)	1594	R	18	-18	58	6.20
			26	-9	70	6.06
			14	11	48	4.64
SUPERIOR FRONTAL GYRUS (BA8)		R	17	15	60	4.79
MIDDLE FRONTAL GYRUS (BA8)		R	32	6	57	4.63
PRECENTRAL GYRUS (BA4)	1037	R	18	-30	70	5.98
POSTCENTRAL GYRUS (BA3)		R	33	-34	63	5.37
INTRAPARIETAL SULCUS (BA40)		R	39	-36	39	4.86
		R	39	-34	46	4.83
ROLANDIC OPERCULUM (BA48)	553	R	53	0	15	6.00
PUTAMEN	325	L	-20	8	13	5.23
INFERIOR FRONTAL GYRUS, P. OPERCULARIS (BA48, BA45)	306	R	39	14	15	5.16
CAUDATE NUCLEUS		R	21	15	12	4.73
POSTERIOR CINGULATE CORTEX (BA27)	295	R	2	-38	9	7.22
SUPERIOR PARIETAL LOBULE (BA5M)	233	R	11	-55	53	5.23
SUPERIOR PARIETAL LOBULE (BA7A)		R	15	-57	59	3.94
INTRAPARIETAL SULCUS (BA19)		R	21	-52	40	4.10
MIDDLE FRONTAL GYRUS (BA47)	184	L	-29	45	19	4.80
LINGUAL GYRUS (BA19)	172	L	-18	-58	-3	5.28

Correlations were considered significant at $p < 0.001$ and corrected for multiple comparisons by FDR at the cluster-level (k = 172; R, right, L, left).

IV. DISCUSSION

We designed and tested an fMRI motor paradigm during which measurements of kinematics and BOLD activity associated with voluntary alternating and repetitive movements of the lower limbs were concurrently recorded in healthy subjects. A custom treadmill-like device was employed in combination with an external visuo-spatial guide to facilitate the synchronization of the subject movement with the timing required in the task. Stepping displacements were registered and quantified, allowing evaluating the correlation of motion amplitude and evoked BOLD activity. Our results demonstrate that stepping generates extensive bilateral activations in several cortical and subcortical brain regions know to be related to motor execution and motor control (see Fig. 5 and Table II). The use of individual kinematic measurements in the fMRI analysis revealed a right lateralized brain network co-varying with inter-subject differences in stepping amplitude (Fig. 6 and Table III).

A. Pseudogait-MRCD

Regarding MR-compatibility, we minimized the impact on the magnetic field by constructing the MRCD mainly from non-ferromagnetic materials. We used standard methods to evaluate MR-compatibility which indicated that the MRCD did not significantly alter the image quality (Fig. 3). This shows the usefulness of the custom-device for registering lower limb displacements in the MR environment while restraining the requested movement to the joints of interest with limited head-motion. In [15], Hollnagel *et al.* presented a MR compatible device which allows to generate and measure passive and active forces related to stepping movements. Both studies represent valuable tools that examine the feasibility of compatible devices in fMRI studies for lower limbs movements.

B. Kinematics

Results revealed that participants matched the visually-cued movements with adequate and precise exertions at the requested timing [Fig. 4(d)], showing an anti-phasing coordination pattern of their lower limbs (Fig. 4(a) and (b) and Supplementary Material, Section II). The timing of the feet contacts were not synchronous with the knee extensions, so the corrections performed by the knee during the consecutive steps were not fully synchronized with the feet-roller displacement. This suggests, despite a close coordinated interlimb relationship, certain autonomy between knee and feet motion.

On the other hand, the option of freely selecting movement amplitude led to inter-subject differences in the SA [Fig. 4(c)] and thus in the TEM. The SA measure was shown to correlate with the subjects' weight but not height. Regarding height, the

lack of correlation is likely explained by the adjustment of the MRCD to each individual's height along the scanner table and the unit of measure being angles. The negative correlation with weight shown in Fig. 4(e) might be due to the subjects being in supine position and could be reflecting gravitational forces that may make the task more tiring for those with greater weights. Nevertheless, stepping lengths are also known to vary greatly between individuals during normal gait [31]. Hence, it would be interesting in future studies to evaluate if the differences in the experimental measurements reflect inter-individual differences in normal walking.

Human walking is considered symmetrical [32], and it is characterized by a cyclical movement governed by an anti-phasing coordination pattern between both limbs. The sensory information derived from alternating leg movements also contributes to the generation and coordination of the muscles during locomotor activity [33]. Likewise, our study incorporated symmetrical movements with a realistic anti-phasing pattern of coordination between both legs since the interaction with the MRCD comprised functionality of the knee, ankle and feet and led to relevant somatosensory feedback. Therefore, the task used in the study was characterized by a well learned movement which may bear high resemblance with a locomotion pattern. However, this task, as a surrogate of gait, is not void of limitations. The goal of locomotion is to support the body against gravity while generating movements which propel the body forward [34]. It is difficult to replicate within a standard fMRI setting specific aspects of gait as the upright stance, balance, weight support and any other gravitational and inertial effects. Other gait components, such as truncal and hip control, or coordination of gluteal and leg muscles with the upper limbs were also limited in our design due to the subject fixations and position. We have tested in a case study some functional evidences between upright and supine stepping with EMG and EMG techniques (Supplementary Material, Section IV).

Despite these clear differences between our task and real walking, the designed MRCD appears as a powerful tool that permits to investigate meaningful aspects of gait within an fMRI scanner.

C. Brain Activation Associated With Stepping

The comparison between motor and resting conditions (SC versus CC) revealed that stepping activates a brain network comprising the primary sensorimotor and somatosensory cortices, SMA, PMC, MC, the basal ganglia and cerebellum (Fig. 5 and Table II). Results are in agreement with previous imaging studies which have assessed brain activity during unilateral [8], [9], [11], [13], [19] and bilateral [14]–[16] lower limb tasks. The individual total extent of movement (TEM) was proven useful as a nuisance covariate that permitted to normalize the functional data in the individual statistical analyses and therefore improved the overall statistical significance of the random-effects group activation maps. This emphasizes the importance of the use of quantitative kinematic measurements in fMRI analyses of motor paradigms.

There is converging evidence about the involvement of an organized network of neural assemblies at spinal and supraspinal levels during coordinated tasks, in which dynamic processes take place to ensure efferent organization and sensory integration [35]. Specifically, M1, SMA, and MC have been shown to participate in encoding aspects related to preparation and execution during voluntary and triggered sequential movements of the upper limbs [17], [35], [36]. Activation of the PMC has also been described in paradigms involving guided-paced movements as opposed to self-paced movements, and may be related to the planning of the movement [37]. Moreover, premotor areas are crucial in processing visual signals for action planning [38] and have also been directly associated with an anti-phasing-coordination behavior: a PET study involving fingers and ankle coordinated movements of opposite limbs proposed a common neural circuitry distributed over the right dorsal PMC and the right parietal cortex to be involved in anti-phasing movements [39]. On the other hand, premotor and posterior parietal areas mediate perception aspects regarding spatial distance estimation and coding of spatial locations relative to body parts, especially in egocentric frame-referencing [40], [41]. The MC may serve as a motivational-motor interface [42] as this area is implicated in processing intentional aspects of movement [7]. Lastly, the basal ganglia and cerebellum have been classically linked to motor control [43]. The basal ganglia have been suggested to participate in time perception and encoding of time intervals [44], [45]. For example, a recent study involving alternating and coordinated leg movements similar to our task, suggested a significant role of the basal ganglia in such movements particularly under self-paced conditions [16]. The areas we found activated with lower limbs repetitive movements in the cerebellum matched the feet somatotopical representation in the upper human cerebellum: an upside-down homunculus [46]. The cerebellum is involved in monitoring and optimizing movements using sensory feedback [47], especially in those that require visuo-motor coordination [48]; activation in the vermis has been observed in studies of repetitive lower-limb movement in either auditory or visual form [7], [9].

Summarizing, the contrast comparing movement and resting conditions led to the functional activation of cortical and subcortical structures that are known to participate in the motor execution and control of voluntary movements. Results support the usefulness and validity of our task as a close model of gait.

D. Brain Activity Correlated With the Stepping Amplitude

We found several brain regions where BOLD signal showed a linear relationship with the SA kinematic regressor (Fig. 6 and Table III). A positive correlation between the BOLD signal and the SA indicates that the subjects with greater stepping amplitudes had higher brain activity in specific areas than those with smaller stepping amplitudes (Fig. 6). We found positive correlation in several cortical and subcortical areas, including the bilateral primary visual and the right extrastriate areas, the lingual gyrus, the right middle temporal complex (hMT/V5+), the right posterior cingulate cortex, the precuneus, the right SPL, the IPL extending to the postcentral gyrus and the bilateral anterior putamen.

The activation found in the striate cortex could be related with attentional visual processing to filter information relevant to the goal-directed behavior or visual demands during the task [49]

whereas extra-striatal regions are supposed to be involved in generating visual predictions relevant to the control of actions [50]: the middle temporal area hMT/V5+ is a major motion sensitive area involved in motion processing [51]. Additionally, the visuo-motor processing of egocentric spatial relations may be mediated by medial superior parietal areas, as the precuneus [52] and areas in the intraparietal sulcus, which have shown a central role in controlling eye and in the generation of visual attention [53]. Moreover, somesthetic egocentric spatial perception has been related to the connectivity between the right SPL (including the precuneus and supramarginal gyrus), the dorsolateral prefrontal cortex and the lingual gyrus [54]. We observed participation of subcortical areas as the bilateral striatum, which has been related with the control of movement extent [55]. Interestingly, the dorsal putamen, which somatotopically corresponds to the lower limb region [56], was correlated with the SA regressor.

Finally, it is worth noting the right lateralization of the activations found. It is generally assumed that the brain exhibits functional asymmetries between hemispheres, i.e., it is accepted that the left hemisphere is dominant for motor control in right-handed individuals while parieto-frontal circuits of the right hemisphere are specialized in attention and spatial processing. Our results are in the agreement with a recent study which suggests that motor performance with visual guidance engages a right-lateralized network to produce well-coordinated behavior on the lower limbs [13]. Overall results suggest that visuo-motor and attentional control mechanisms could be employed to produce a coordinated motor behavior, which may be mainly mediated by striatal, extra-striatal, and fronto-parietal areas.

In conclusion, the use of a custom-designed MRCD, together with the concurrent measurement of the subject motor behavior proved relevant to retrieving nonartifacted BOLD images that reflected the actual movement performed by the volunteers inside the scanner. Furthermore, this design allowed a detailed analysis of the individual performance based on kinematic features. Overall, the combination of fMRI and kinematics analysis of performance along the scanning session offers a great potential for the study of the brain motor systems and their disorders.

ACKNOWLEDGMENT

The authors would like to thank Dr. Valencia, Dr. Alegre, and Dr. Artieda for the assistance during the analyses of the EEG and EMG recordings (Supplementary Material, Section IV).

REFERENCES

[1] S. Rossignol, R. Dubuc, and J.-P. Gossard, "Dynamic sensorimotor interactions in locomotion," *Physiol. Rev.*, vol. 86, no. 1, pp. 89–154, Jan. 2006.

[2] I. Miyai, H. C. Tanabe, I. Sase, H. Eda, I. Oda, I. Konishi, Y. Tsunazawa, T. Suzuki, T. Yanagida, and K. Kubota, "Cortical mapping of gait in humans: A near-infrared spectroscopic topography study," *Neuroimage*, vol. 14, no. 5, pp. 1186–1192, Nov. 2001.

[3] K. Jahn, A. Deutschländer, T. Stephan, M. Strupp, M. Wiesmann, and T. Brandt, "Brain activation patterns during imagined stance and locomotion in functional magnetic resonance imaging," *Neuroimage*, vol. 22, no. 4, pp. 1722–1731, Aug. 2004.

[4] K. Sacco, F. Cauda, L. Cerliani, D. Mate, S. Duca, and G. C. Geminiani, "Motor imagery of walking following training in locomotor attention. The effect of 'the tango lesson'," *Neuroimage*, vol. 32, no. 3, pp. 1441–1449, Sep. 2006.

[5] M. Bakker, C. C. P. Verstappen, B. R. Bloem, and I. Toni, "Recent advances in functional neuroimaging of gait," *J. Neural Transmiss.*, vol. 114, no. 10, pp. 1323–1331, Jul. 2007.

[6] C. la Fougère, A. Zwergal, A. Rominger, S. Förster, G. Fesl, M. Dieterich, T. Brandt, M. Strupp, P. Bartenstein, and K. Jahn, "Real versus imagined locomotion: A [18F]-FDG PET-fMRI comparison," *Neuroimage*, vol. 50, no. 4, pp. 1589–1598, May 2010.

[7] F. Debaere, S. P. Swinnen, E. Béatse, S. Sunaert, P. Van Hecke, and J. Duysens, "Brain areas involved in interlimb coordination: A distributed network," *Neuroimage*, vol. 14, no. 5, pp. 947–958, Nov. 2001.

[8] B. H. Dobkin, A. Firestine, M. West, K. Saremi, and R. Woods, "Ankle dorsiflexion as an fMRI paradigm to assay motor control for walking during rehabilitation," *Neuroimage*, vol. 23, no. 1, pp. 370–381, Sep. 2004.

[9] C. Sahyoun, A. Floyer-Lea, H. Johansen-Berg, and P. M. Matthews, "Towards an understanding of gait control: Brain activation during the anticipation, preparation and execution of foot movements," *Neuroimage*, vol. 21, no. 2, pp. 568–575, Feb. 2004.

[10] E. Kapreli, S. Athanasopoulos, M. Papathanasiou, P. Van Hecke, N. Strimpakos, A. Gouliamos, R. Peeters, and S. Sunaert, "Lateralization of brain activity during lower limb joints movement. An fMRI study," *Neuroimage*, vol. 32, no. 4, pp. 1709–1721, Oct. 2006.

[11] J. M. Newton, Y. Dong, J. Hidler, P. Plummer-D'Amato, J. Marehbian, R. M. Albistegui-Dubois, R. P. Woods, and B. H. Dobkin, "Reliable assessment of lower limb motor representations with fMRI: Use of a novel MR compatible device for real-time monitoring of ankle, knee and hip torques," *Neuroimage*, vol. 43, no. 1, pp. 136–146, Oct. 2008.

[12] S. Francis, X. Lin, S. Aboushoushah, T. P. White, M. Phillips, R. Bowtell, and C. S. Constantinescu, "fMRI analysis of active, passive and electrically stimulated ankle dorsiflexion," *Neuroimage*, vol. 44, no. 2, pp. 469–479, Jan. 2009.

[13] D. G. Woolley, N. Wenderoth, S. Heuninckx, X. Zhang, D. Callaert, and S. P. Swinnen, "Visual guidance modulates hemispheric asymmetries during an interlimb coordination task," *Neuroimage*, vol. 50, no. 4, pp. 1566–1577, May 2010.

[14] J. P. Mehta, M. D. Verber, J. A. Wieser, B. D. Schmit, and S. M. Schindler-Ivens, "A novel technique for examining human brain activity associated with pedaling using fMRI," *J. Neurosci. Methods*, vol. 179, no. 2, pp. 230–239, May 2009.

[15] C. Hollnagel, M. Brügger, H. Vallery, P. Wolf, V. Dietz, S. Kollias, and R. Riener, "Brain activity during stepping: A novel MRI-compatible device," *J. Neurosci. Methods*, vol. 201, no. 1, pp. 124–130, Sept. 2011.

[16] A. Toyomura, M. Shibata, and S. Kuriki, "Self-paced and externally triggered rhythmical lower limb movements: A functional MRI study," *Neurosci. Lett.*, vol. 516, no. 1, pp. 39–44, May 2012.

[17] J. Ashe and K. Ugurbil, "Functional imaging of the motor system," *Curr. Opin. Neurobiol.*, vol. 4, no. 6, pp. 832–839, Dec. 1994.

[18] S. M. Rao, P. A. Bandettini, J. R. Binder, J. A. Bobholz, T. A. Hammeke, E. A. Stein, and J. S. Hyde, "Relationship between finger movement rate and functional magnetic resonance signal change in human primary motor cortex," *J. Cereb. Blood Flow Metab.*, vol. 16, no. 6, pp. 1250–1254, Nov. 1996.

[19] O. Ciccarelli, A. T. Toosy, J. F. Marsden, C. M. Wheeler-Kingshott, C. Sahyoun, P. M. Matthews, D. H. Miller, and A. J. Thompson, "Identifying brain regions for integrative sensorimotor processing with ankle movements," *Exp. Brain Res.*, vol. 166, no. 1, pp. 31–42, Sep. 2005.

[20] G. Taubin, "Estimation of planar curves, surfaces, and nonplanar space curves defined by implicit equations with applications to edge and range image segmentation," *IEEE Trans. Pattern Anal. Mach. Intell.*, vol. 13, no. 11, pp. 1115–1138, Nov. 1991.

[21] N. Yu, R. Gassert, and R. Riener, "Mutual interferences and design principles for mechatronic devices in magnetic resonance imaging," *Int. J. Comput. Assist. Radiol. Surg.*, vol. 6, no. 4, pp. 473–488, Jul. 2011.

[22] L. Kaufman, D. M. Kramer, L. E. Crooks, and D. A. Ortendahl, "Measuring signal-to-noise ratios in MR imaging," *Radiology*, vol. 173, no. 1, pp. 265–267, Oct. 1989.

[23] R. C. Oldfield, "The assessment and analysis of handedness: The Edinburgh inventory," *Neuropsychologia*, vol. 9, no. 1, pp. 97–113, Mar. 1971.

[24] K. J. Friston, S. Williams, R. Howard, R. S. J. Frackowiak, and R. Turner, "Movement related effects in fMRI time series," *Magn. Res. Med.*, vol. 35, pp. 346–355, 1996.

[25] P. Mazaika, F. Hoefl, G. H. Glover, and A. L. Reiss, "Methods and software for fMRI analysis for clinical subjects," *Human Brain Mapp.*, 2009.

[26] V. Fonov, A. C. Evans, K. Botteron, C. R. Almli, R. C. McKinstry, and D. L. Collins, "Unbiased average age-appropriate atlases for pediatric studies," *Neuroimage*, vol. 54, no. 1, pp. 313–327, Jan. 2011.
[27] J. Ashburner and K. J. Friston, "Unified segmentation," *Neuroimage*, vol. 26, no. 3, pp. 839–851, July 2005.
[28] K. J. Friston, C. D. Frith, R. Turner, and R. S. J. Frackowiak, "Characterizing evoked hemodynamics with fMRI," *NeuroImage*, vol. 2, no. 2, pp. 157–165, 1995.
[29] T. Johnstone, K. S. O. Walsh, L. L. Greischar, A. L. Alexander, A. S. Fox, R. J. Davidson, and T. R. Oakes, "Motion correction and the use of motion covariates in multiple-subject fMRI analysis," *Human Brain Mapp.*, vol. 27, no. 10, pp. 779–788, Oct. 2006.
[30] W. D. Penny and A. J. Holmes, "Random effects analysis," in *Human Brain Function II*, R. S. J. Frackowiack, K. J. Friston, C. D. Frith, R. Dolan, C. J. Price, J. Ashburner, W. Penny, and S. Zeki, Eds., 2nd ed. San Diego, CA: Elsevier, 2004.
[31] J. M. Hausdorff, Y. Ashkenazy, C. K. Peng, P. C. Ivanov, H. E. Stanley, and A. L. Goldberger, "When human walking becomes random walking: Fractal analysis and modeling of gait rhythm fluctuations," *Physica A*, vol. 302, no. 1–4, pp. 138–147, Dec. 2001.
[32] H. Sadeghi, P. Allard, F. Prince, and H. Labelle, "Symmetry and limb dominance in able-bodied gait: A review," *Gait Posture*, vol. 12, no. 1, pp. 34–45, Sep. 2000.
[33] N. Kawashima, D. Nozaki, M. O. Abe, M. Akai, and K. Nakazawa, "Alternate leg movement amplifies locomotor-like muscle activity in spinal cord injured persons," *J. Neurophysiol.*, vol. 93, no. 2, pp. 777–785, Feb. 2005.
[34] D. A. Winter, "Human balance and posture control during standing and walking," *Gait Posture*, vol. 3, no. 4, pp. 193–214, 1995.
[35] S. P. Swinnen, "Intermanual coordination: From behavioural principles to neural-network interactions," *Nat. Rev. Neurosci.*, vol. 3, no. 5, pp. 348–359, May 2002.
[36] T. Dai, J. Liu, V. Sahgal, R. Brown, and G. Yue, "Relationship between muscle output and functional MRI-measured brain activation," *Exp. Brain Res.*, vol. 140, no. 3, pp. 290–300, 2001.
[37] K. Wessel, T. Zeffiro, C. Toro, and M. Hallett, "Self-paced versus metronome-paced finger movements. A positron emission tomography study," *J. Neuroimag.*, vol. 7, no. 3, pp. 145–151, Jul. 1997.
[38] E. Hoshi and J. Tanji, "Differential involvement of neurons in the dorsal and ventral premotor cortex during processing of visual signals for action planning," *J. Neurophysiol.*, vol. 95, no. 6, pp. 3596–3616, Jun. 2006.
[39] B. M. de Jong, K. L. Leenders, and A. M. J. Paans, "Right parieto-premotor activation related to limb-independent antiphase movement," *Cereb. Cortex*, vol. 12, no. 11, pp. 1213–1217, Nov. 2002.
[40] G. Vallar, E. Lobel, G. Galati, A. Berthoz, L. Pizzamiglio, and D. Le Bihan, "A fronto-parietal system for computing the egocentric spatial frame of reference in humans," *Exp. Brain Res.*, vol. 124, no. 3, pp. 281–286, Feb. 1999.
[41] G. Committeri, G. Galati, A.-L. Paradis, L. Pizzamiglio, A. Berthoz, and D. LeBihan, "Reference frames for spatial cognition: Different brain areas are involved in viewer-, object-, and landmark-centered judgments about object location," *J. Cognit. Neurosci.*, vol. 16, no. 9, pp. 1517–1535, Nov. 2004.
[42] T. Ball, A. Schreiber, B. Feige, M. Wagner, C. H. Lücking, and R. Kristeva-Feige, "The role of higher-order motor areas in voluntary movement as revealed by high-resolution EEG and fMRI," *Neuroimage*, vol. 10, no. 6, pp. 682–694, Dec. 1999.
[43] F. A. Middleton and P. L. Strick, "Basal ganglia and cerebellar loops: Motor and cognitive circuits," *Brain Res. Rev.*, vol. 31, no. 2–3, pp. 236–250, 2000.
[44] S. M. Rao, A. R. Mayer, and D. L. Harrington, "The evolution of brain activation during temporal processing," *Nat. Neurosci.*, vol. 4, no. 3, pp. 317–323, Mar. 2001.
[45] M. A. Pastor, B. L. Day, E. Macaluso, K. J. Friston, and R. S. J. Frackowiak, "The functional neuroanatomy of temporal discrimination," *J. Neurosci.*, vol. 24, no. 10, pp. 2585–2591, Mar. 2004.
[46] W. Grodd, E. Hülsmann, M. Lotze, D. Wildgruber, and M. Erb, "Sensorimotor mapping of the human cerebellum: fMRI evidence of somatotopic organization," *Hum. Brain Mapp.*, vol. 13, no. 2, pp. 55–73, Jun. 2001.
[47] M. Jueptner and C. Weiller, "A review of differences between basal ganglia and cerebellar control of movements as revealed by functional imaging studies," *Brain*, vol. 121, pp. 1437–1449, Aug. 1998.
[48] J. F. Stein and M. Glickstein, "Role of the cerebellum in visual guidance of movement," *Physiol. Rev.*, vol. 72, no. 4, pp. 967–1017, Oct. 1992.
[49] M. Corbetta and G. L. Shulman, "Control of goal-directed and stimulus-driven attention in the brain," *Nat. Rev. Neurosci.*, vol. 3, no. 3, pp. 201–215, Mar. 2002.
[50] S. V. Astafiev, C. M. Stanley, G. L. Shulman, and M. Corbetta, "Extrastriate body area in human occipital cortex responds to the performance of motor actions," *Nat. Neurosci.*, vol. 7, no. 5, pp. 542–548, May 2004.
[51] S. Sunaert, P. Van Hecke, G. Marchal, and G. A. Orban, "Motion-responsive regions of the human brain," *Exp. Brain Res.*, vol. 127, no. 4, pp. 355–370, Aug. 1999.
[52] T. Zaehle, K. Jordan, T. Wüstenberg, J. Baudewig, P. Dechent, and F. W. Mast, "The neural basis of the egocentric and allocentric spatial frame of reference," *Brain Res.*, vol. 1137, no. 1, pp. 92–103, Mar. 2007.
[53] J. W. Bisley and M. E. Goldberg, "Neuronal activity in the lateral intraparietal area and spatial attention," *Science*, vol. 299, no. 5603, pp. 81–86, Jan. 2003.
[54] F. R. Loayza, M. A. Fernández-Seara, M. Aznárez-Sanado, and M. A. Pastor, "Right parietal dominance in spatial egocentric discrimination," *NeuroImage*, vol. 55, no. 2, pp. 635–643, 2011.
[55] R. S. Turner, S. T. Grafton, J. R. Votaw, M. R. Delong, and J. M. Hoffman, "Motor subcircuits mediating the control of movement velocity: A PET study," *J. Neurophysiol.*, vol. 80, no. 4, pp. 2162–2176, Oct. 1998.
[56] E. Gerardin, S. Lehéricy, J. B. Pochon, S. T. du Montcel, J. F. Mangin, F. Poupon, Y. Agid, D. Le Bihan, and C. Marsault, "Foot, hand, face and eye representation in the human striatum," *Cereb. Cortex*, vol. 13, no. 2, pp. 162–169, 2003.